Ligand Geometry of the Ternary Complex of 5-Enolpyruvylshikimate-3-phosphate Synthase from Rotational-Echo Double-Resonance NMR†

Lynda M. McDowell,‡ Christopher A. Klug,‡,§ Denise D. Beusen,‖,⊥ and Jacob Schaefer*,‡

Department of Chemistry and Center for Molecular Design, Institute for Biomedical Computing, Washington University, St. Louis, Missouri 63130

Received December 11, 1995⊗

ABSTRACT: The 46-kDa enzyme 5-enolpyruvylshikimate-3-phosphate (EPSP) synthase catalyzes the condensation of shikimate 3-phosphate (S3P) and phosphoenolpyruvate (PEP) to form EPSP. The reaction is inhibited by *N*-(phosphonomethyl)glycine (Glp), which, in the presence of S3P, binds to EPSP synthase to form a stable ternary complex. As part of a solid-state NMR characterization of this structure, we have used dipolar recovery at the magic angle (DRAMA) and rotational-echo double resonance (REDOR) to determine intra- and interligand internuclear distances. DRAMA was used to determine the single $^{31}P-^{31}P$ distance, while REDOR was used to determine one $^{31}P-^{15}N$ distance and five $^{31}P-^{13}C$ distances. These experimental distances were used as restraints in molecular dynamics simulations of an S3P−Glp complex to examine the geometry of the two ligands relative to one another in the ternary complex. The simulations were compared to unrestrained simulations of the EPSP synthase tetrahedral intermediate and its phosphonate analog. The results suggest that Glp is unlikely to bind in the same fashion as PEP, a conclusion that is consistent with recent studies that have questioned the role of Glp as a transition-state or intermediate analog.

The 46-kDa enzyme 5-enolpyruvylshikimate-3-phosphate (EPSP)[1] synthase catalyzes the reversible condensation of shikimate 3-phosphate (S3P) and phosphoenolpyruvate (PEP) to form EPSP in the synthesis of aromatic amino acids in plants and microorganisms (Steinrucken & Amrhein, 1984a; Anderson & Johnson, 1990). This reaction is inhibited by the commercial herbicide *N*-(phosphonomethyl)glycine (glyphosate or Glp), $HO_3PCH_2NHCH_2COOH$, which, in the presence of S3P, binds to EPSP synthase (EPSPS) and forms a stable, ternary complex (Steinrucken & Amrhein, 1984b; Anderson et al., 1988a). A crystal structure of unliganded EPSP synthase has been published (Stallings et al., 1991), but there is no structure available for the ternary complex, which apparently does not form crystals suitable for diffraction studies. The crystal structure of unliganded EPSP synthase reveals two domains separated by a cleft which is presumably the region of the binding site.

Our strategy for the NMR characterization of the ternary complex is in four parts. The first part of our strategy is reported in this paper. Carbon-13 and ^{15}N labels were placed in Glp, and distances were measured using rotational-echo, double-resonance (REDOR) NMR from these labels to ^{31}P in S3P and Glp. The measurements were performed on a ternary complex that had been frozen from dilute solution and lyophilized. Each EPSPS−S3P−Glp complex was surrounded by at least 50 buffer molecules so that the complex was immobilized in an ionic glass formed by the freeze-quenched buffer. Formation of the glass inhibits crystallization of ice within the binding site and prevents aggregation of the protein. Homogeneity of charge-stabilized binding sites of protein complexes embedded in ionic glasses with preserved native geometry has been observed in our laboratory for EPSP synthase (Christensen & Schaefer, 1993), *Escherichia coli* glutamine binding protein (Hing et al., 1994), and ribulose-1,5-bisphosphate carboxylase (Mueller et al., 1995). Distances resulting from inter- and intraligand EPSPS REDOR measurements help to define the geometry of the two substrates relative to one another. Some results from this phase of the work have been described already (Christensen & Schaefer, 1993; McDowell et al., 1993; Beusen et al., 1994).

The second part of our strategy (Beusen et al., 1994; Schaefer, 1995; McDowell et al., 1996) involves the introduction of ^{15}N labels into the lysine, arginine, and histidine residues of EPSP synthase to determine which are near the ^{31}P of the negatively charged phosphate of S3P and the negatively charged carboxyl and phosphonate groups of Glp. The protein labeling was done using an *E. coli* expression system capable of producing 100 mg of purified protein from 1 L of defined media containing 100 mg/L ^{15}N-labeled amino acid. The third part of the strategy uses mutagenesis to locate ^{19}F-labeled tryptophans in the upper and lower domains of EPSPS and long-range $^{19}F-^{31}P$ REDOR distance determinations to measure directly the extent to which the cleft closes around ^{31}P-containing ligands (Studelska et al., 1996). The fourth part of our strategy will use all the interatomic distances determined by DRAMA and REDOR as restraints in molecular dynamics simulations to build a full model of the ternary complex.

† This work was supported by NIH Grant GM-40634.

‡ Department of Chemistry.

§ Present address: Department of Chemical Engineering, Stanford University, Stanford, CA 94305.

‖ Institute for Biomedical Computing.

⊥ Present address: Tripos, Inc., St. Louis, MO 63144.

⊗ Abstract published in *Advance ACS Abstracts,* April 1, 1996.

[1] Abbreviations: EPSP, 5-enolpyruvylshikimate 3-phosphate; EPSPS, 5-enolpyruvylshikimate-3-phosphate synthase; S3P, shikimate 3-phosphate; PEP, phosphoenolpyruvate; Glp, *N*-(phosphonomethyl)glycine; DRAMA, dipolar recovery at the magic angle; REDOR, rotational-echo double resonance; IC_{50}, inhibitory ligand concentration that reduces enzyme activity by 50%.

S0006-2960(95)02905-9 CCC: $12.00

MATERIALS AND METHODS

Growth of Wild-Type E. coli for Production of EPSP Synthase. EPSP synthase was isolated from an *E. coli* construct, W3110/pMON5537, which overproduces the enzyme. This strain was provided by Alan Easton of Monsanto Co. (St. Louis, MO). Details of the medium and growth conditions have been presented (Christensen & Schaefer, 1993).

Purification and Complexation. EPSP synthase purification was as described (Christensen & Schaefer, 1993) except an additional fast-flow Q-Sepharose column (2.5 × 15 cm) was run after the phenyl-Sepharose column. The Q-Sepharose elution used a 500 mL linear gradient from buffer C (25 mM Tris, pH 7.5, 25 mM KCl, 5 mM β-mercaptoethanol) to buffer D (25 mM Tris, pH 7.5, 400 mM KCl, 5 mM β-mercaptoethanol) and a 10 mL/min flow rate. After concentration by ultrafiltration, 10% (by volume) glycerol was added and the enzyme was stored at −80 °C. Prior to lyophilization, EPSP synthase was (i) exchanged into 2 mM MOPS (4-morpholinepropanesulfonic acid), pH 7.2, 1 mM dithiothreitol, and 10 μM EDTA, (ii) diluted to 50 μM (2.28 mg/mL), (iii) incubated for about 1 h at room temperature with 25% excess S3P and 10% excess of the appropriate glyphosate, and (iv) shell-frozen using a liquid nitrogen bath. Samples appeared dry after overnight lyophilization but typically remained on the lyophilizer for 1 or 2 more days. Final water content was approximately 20% by weight. Four different glyphosates were used: [1-^{13}C]Glp (99% ^{13}C, Merck Stable Isotopes), [2-^{13}C]Glp (99% ^{13}C, Isotec), [3-^{13}C,^{15}N]-Glp (90% ^{13}C, 99% ^{15}N, Merck Stable Isotopes), and natural-abundance glyphosate (J. Sikorski, Monsanto Co.). The ternary complexes with [3-^{13}C,^{15}N]Glp and with natural-abundance Glp each contained 200 mg of EPSP synthase (total sample weight of 320 mg). The complexes with [1-^{13}C]Glp and [2-^{13}C]Glp contained 170 and 145 mg of EPSP synthase, respectively.

DRAMA. Dipolar restoration at the magic angle (DRAMA) uses rotor-synchronized 90° pulses to dephase the magnetization of isolated homonuclear pairs of dipolar-coupled spin-$^1/_2$ nuclei. DRAMA is suitable for measuring the dipolar coupling between the phosphate ^{31}P of S3P and the phosphonate ^{31}P of Glp. The full DRAMA sequence is shown in Figure 1. We begin with a cross-polarization transfer from an abundant proton system. The protons are then decoupled for the remainder of the experiment. A rotor-synchronized Hahn echo is produced on even-numbered rotor cycles by a refocusing π pulse following the completion of odd-numbered cycles (Figure 1a). These π pulses are phase alternated (Gullion et al., 1990) following the XY8 scheme (xyxyyxyx). A complete phase cycle therefore requires 16 rotor cycles. The phase of the leading pulse of the XY8 sequence is determined by the ^{31}P spin quadrature routing.

The frequency-offset dependence of DRAMA due to chemical shift tensors is removed (Klug et al., 1994) using eight equally spaced π pulses per rotor cycle (Figure 1b). These pulses are placed at $^1/_{16}$, $^3/_{16}$, $^5/_{16}$, ... of the rotor period (T_r). The phases of these π pulses are also alternated according to the XY8 scheme. Phase accumulation at the spinning frequency and twice the spinning frequency from chemical shift interactions for transverse magnetization arising from individual crystallites in an isotropic powder cancel under the four sign reversals created in each half-rotor cycle by the eight π pulses. The DRAMA ^{31}P full echo which forms at the completion of even numbers of rotor cycles using the sequence of Figure 1b is S_0. Two 90° pulses per rotor period are placed at $^1/_4$ and $^3/_4$ T_r for maximum dephasing (Figure 1c). These pulses all have the same phase which is determined by the ^{31}P quadrature routing. The DRAMA-dephased echo which forms at the completion of even numbers of rotor cycles using the sequence of Figure 1c is S. The ^{31}P DRAMA difference is $\Delta S = S_0 - S$.

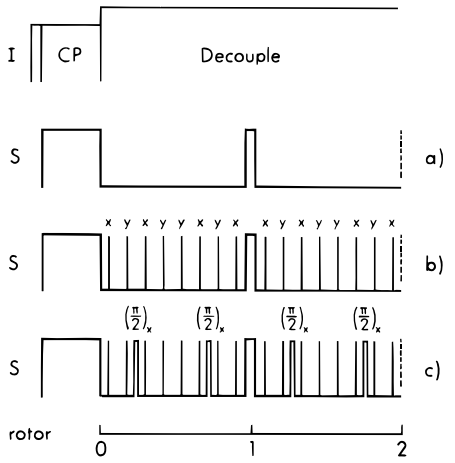

FIGURE 1: Pulse sequences for an $I-S$ matched spin-lock, cross-polarization transfer (with spin-temperature alternation) followed by (a) a rotor-synchronized S-spin Hahn echo, (b) a compensated DRAMA full echo, and (c) a compensated DRAMA-dephased echo. The I and S labels in the figure identify abundant and rare spins, respectively. Phase alternation of the refocusing Hahn π pulse after odd-numbered rotor cycles, and of the eight equally spaced π pulses during each rotor period of the compensated DRAMA sequences, follows the XY8 scheme. All dephasing $\pi/2$ pulses have the same phase. The illustration is for two rotor cycles.

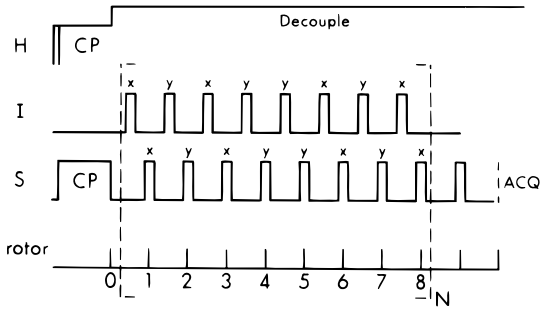

FIGURE 2: REDOR pulse sequence with π pulses on both I and S channels. The I and S labels in the figure identify two types of rare spins. The pulses are applied using an XY8 phase-cycling scheme to suppress the effects of frequency offsets and compensate for pulse imperfections. Signal acquisition begins two rotor cycles after the completion of a full $8N$ rotor cycles of dephasing. The two extra rotor cycles (and a Hahn-echo refocusing pulse) ensure that the start of data acquisition is not coincident with a pulse. A full-echo signal, S_0, is obtained by omitting the I-spin dephasing pulses. The dephased signal is S. The REDOR difference is $\Delta S = S_0 - S$.

REDOR. REDOR provides a direct measure of heteronuclear dipolar coupling between isolated pairs of labeled nuclei (Gullion & Schaefer, 1989a,b). In a solid with a ^{31}P−^{13}C-labeled spin pair, for example, the ^{31}P rotational echoes that form each rotor period following a proton to ^{31}P (S spin in Figure 2) cross-polarization transfer are prevented from reaching full intensity by insertion of ^{13}C π pulses (^{13}C is the I spin in Figure 2). The pulses are applied using the XY8 phase-cycling scheme (Gullion et al., 1990; Gullion & Schaefer, 1991) described above to suppress offset effects

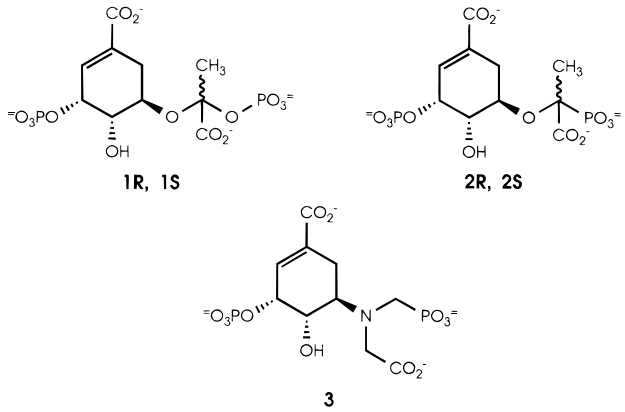

FIGURE 3: Structures of EPSP synthase intermediates and inhibitors: **1**, EPSP synthase tetrahedral intermediate; **2**, phosphonate intermediate analog; **3**, S3P−Glp bisubstrate analog.

and help compensate for pulse imperfections. Signal acquisition begins two rotor cycles after the completion of a full 8*N* rotor cycles of dephasing. The REDOR difference (the difference between a ^{31}P NMR spectrum obtained under these conditions and one obtained with no ^{13}C π pulses) has a strong dependence on the dipolar coupling and hence the internuclear distance (Gullion & Schaefer, 1989b). The dephasing of magnetization in REDOR arises from a local dipolar field gradient and involves no polarization transfer. REDOR has no dependence on ^{31}P or ^{13}C chemical shift tensors and does not require resolution of a ^{31}P−^{13}C coupling in the chemical shift dimension (Marshall et al., 1990; Holl et al., 1992).

Solid-State NMR Spectrometer. Lyophilized samples were packed into high-performance 7.5-mm outside-diameter zirconia rotors fitted with Kel-F spacers and a drive cap. Cross-polarization, magic-angle spinning spectra were obtained at 7.05 T using a Chemagnetics console (Fort Collins, CO) and a four-channel probe (Holl et al., 1990) with a single 9-mm diameter solenoidal coil which permits ^{1}H, ^{31}P, ^{13}C, and ^{15}N detection or dephasing at 300, 121, 75, and 30 MHz, respectively. REDOR experiments began with 1-ms matched spin-lock cross-polarization transfers from protons at 50 kHz followed by proton decoupling at 90 kHz. The sequence repetition time for all experiments was 2 s. The magic-angle stators were obtained from Chemagnetics (Fort Collins, CO). A controlled spinning speed of 4167 Hz was used for DRAMA experiments and 5000 Hz for REDOR experiments.

Molecular Modeling. Energy minimizations and molecular dynamics simulations were done within SYBYL (Tripos, Inc., St. Louis, MO) using the Tripos force field (Clark et al., 1989). The highly charged nature of the ligands and the inhomogeneous dielectric of the protein surrounding them made treatment of electrostatics for simulations involving only ligands problematic. Consequently, charges were not considered in any of the calculations. A convergence criterion of 0.05 kcal/(mol·Å^2) was implemented in the minimizations.

Starting coordinates for *R* and *S* forms of the EPSP synthase tetrahedral intermediate (**1**, Figure 3), the *R* and *S* forms of the phosphonate intermediate analog (**2**, Figure 3), and an S3P−Glp bisubstrate analog (**3**, Figure 3) were built from the reported X-ray structure for shikimate (Abell et al., 1988) using the sketching tools within SYBYL. Starting coordinates for Glp were taken from a reported X-ray structure (Knuuttila & Knuuttila, 1979). The energy for each

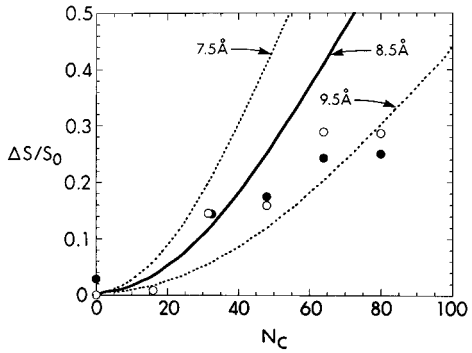

FIGURE 4: DRAMA ^{31}P $\Delta S/S_0$ for a ternary complex of EPSP synthase spinning at the magic angle at 4167 Hz as a function of the number of rotor cycles of dephasing, N_c. A full-echo signal, S_o, is obtained by omitting the $\pi/2$ dephasing pulses (Figure 1b), while the dephased signal, *S*, is obtained by including the $\pi/2$ dephasing pulses (Figure 1c). The DRAMA difference is $\Delta S = S_0 - S$. Both *S* and S_0 spectra for each value of N_c were the result of the accumulation of approximately 10 000 scans. Symbols: open circles, S3P; closed circles, glyphosate.

molecule was minimized as described above. The complex of S3P and Glp was constructed by manually docking the two molecules to match approximately the REDOR and DRAMA distances and then minimizing the energy of the pair using distance restraints. The N of glyphosate was modeled as a quaternary center, in keeping with an earlier report (Castellino et al., 1989) on its protonation when bound in the ternary complex. The restraints were implemented as flat-well exponentials with a force constant of 50 kcal/(mol·Å^2) and an exponent of 2. The error estimates of the DRAMA and REDOR experiments were used to define the width of the flat well.

Molecular dynamics simulations (NTV ensemble; temperature coupling every 10 fs; nonbonded update every 25 fs) were done for 50 ps at both 300K and 500K. Snapshots were recorded every 100 fs. Snapshots from the last 30 ps of each run were energy minimized as described above. In the case of the S3P−Glp complex, restraints were implemented during the dynamics and subsequent energy minimization as described above. Energy-minimized conformers of **1R**, **1S**, **2R**, **2S**, and **3** were screened to identify unique conformers by performing an all-atom, root-mean-square fit of each conformer against all others. Only conformers which differed from the rest by at least 0.5 root-mean-square standard deviations were retained. Interatomic distances in energy-minimized conformers and complexes were recorded using the Molecular Spreadsheet within SYBYL.

RESULTS AND DISCUSSION

DRAMA. The homonuclear dephasing of the glyphosate phosphonate ^{31}P and the S3P phosphate ^{31}P is shown in Figure 4 as a function of the number of rotor cycles of dephasing, N_c. The solid curve is calculated for a ^{31}P−^{31}P distance of 8.5 Å and provides a reasonable match to the data up to $N_c = 40$, where the DRAMA results are most reliable (Klug et al., 1994). All the experimental results can be accounted for by assuming an uncertainty in the distance of ±1 Å (Figure 4, dotted lines).

^{31}P REDOR with ^{15}N Dephasing. The ^{31}P REDOR NMR spectra of EPSPS−S3P−[3-^{13}C,^{15}N]Glp show almost com-

plete dephasing for the glyphosate ^{31}P line after 80 rotor cycles of dephasing (Figure 5, left). The two-bond ^{31}P−^{15}N distance is 2.73 Å (Knuuttila & Knuuttila, 1979), which corresponds to a dipolar coupling of 216 Hz and an expected $\Delta S/S_0$ of 1.0. The observed dephasing for the S3P ^{31}P line is much smaller but still clearly detectable. The $\Delta S/S_0$ is 0.042. The contribution to this dephasing by natural-abundance ^{15}N in the protein can be no more than 0.019 (Figure 5, right). We therefore estimate that the $\Delta S/S_0$ due to label is 0.023, which corresponds to a dipolar coupling of 9.4 Hz and a distance between S3P ^{31}P and glyphosate ^{15}N of 8.0 ± 1 Å.

^{31}P REDOR with ^{13}C Dephasing. Interpretation of the ^{31}P REDOR NMR spectra in terms of positions of the ^{13}C labels is complicated by the substantial natural-abundance background ^{13}C contributions to $\Delta S/S_0$. There are on the order of 50 carbon atoms within the 10-Å dephasing range of the S3P and glyphosate phosphorus nuclei (Stallings et al., 1991). Dephasing of a ^{31}P signal by a ^{13}C label and a natural-abundance ^{13}C depends on the orientation of the two ^{31}P−^{13}C dipolar tensors. As a first approximation we ignore ^{13}C−^{13}C couplings and assume that for an unlabeled system with ^{31}P observation

$$(\Delta S/S_0)_{\text{nat abnd}} = 1 - \langle \cos(\Delta\phi_{\text{nat abnd}}) \rangle_{\text{spin and space}} \quad (1)$$

where $\Delta\phi_{\text{nat abnd}}$ is the REDOR phase accumulation (Gullion & Schaefer, 1989a) resulting from an average coupling between the observed ^{31}P spin and the various natural-abundance ^{13}C dephasing centers in the powder. The bracket indicates an average over both spin and space coordinates. Then, for a system with ^{31}P observation and REDOR dephasing by a single ^{13}C label plus a natural-abundance ^{13}C background

$$(\Delta S/S_0)_{\text{obsd}} = 1 - \langle \cos(\Delta\phi_{\text{D}} + \Delta\phi_{\text{nat abnd}}) \rangle_{\text{spin and space}} \quad (2)$$

$$= 1 - \langle \cos\Delta\phi_{\text{D}} \cos\Delta\phi_{\text{nat abnd}} \rangle_{\text{space}} \quad (3)$$

$$\approx 1 - \langle \cos\Delta\phi_{\text{D}} \rangle_{\text{space}} \langle \cos\Delta\phi_{\text{nat abnd}} \rangle_{\text{space}} \quad (4)$$

where $\Delta\phi_{\text{D}}$ is the REDOR phase accumulation arising from the coupling between the observed ^{31}P spin and the single ^{13}C label. The average over spin coordinates in eq 2 includes dephasing by ^{31}P−^{13}C spin pairs that are either parallel (positive $\Delta\phi_{\text{D}}$) or antiparallel (negative $\Delta\phi_{\text{D}}$). In going from eq 2 to eq 3, we take advantage of the additivity of arguments for the products of exponentials (Boyce, 1972). This is a standard averaging procedure in SEDOR calculations for multiple dephasing spins (Wang et al., 1984). In going from eq 3 to eq 4, we assume independent dephasing by label and background. We perform the first powder average in eq 4 to obtain (Mueller, 1995)

$$\langle \cos\Delta\phi_{\text{D}} \rangle_{\text{space}} \approx 1 - 16\lambda_{\text{D}}^2/15 \quad (5)$$

with

$$\lambda_{\text{D}} = N_{\text{c}} T_{\text{r}} D \quad (6)$$

and

$$D = \gamma_{\text{C}}\gamma_{\text{P}} h/4\pi^2 r^3 \quad (7)$$

where N_{c} is the number of rotor cycles of dephasing, T_{r} is the rotor period, D is the dipolar coupling in hertz, γ_{C} and γ_{P} are the carbon and phosphorus gyromagnetic ratios, respectively, h is Planck's constant, and r is the ^{13}C−^{31}P internuclear distance. Combining eqs 1, 4, and 5, we find that

$$\lambda_{\text{D}}^2 = (15/16)(1 - [1 - (\Delta S/S_0)_{\text{obsd}}]/[1 - (\Delta S/S_0)_{\text{nat abnd}}]) \quad (8)$$

Thus, using eq 8, which is not exact, we determine the approximate dipolar coupling, and hence the distance, between the observed REDOR center and the dephasing ^{13}C label in the presence of the surrounding natural-abundance ^{13}C background. When $\Delta S/S_0$ for both background and label-plus-background are small, eq 8 is equivalent to a simple subtraction of background dephasing (Hing et al., 1994).

REDOR dephasing of glyphosate ^{31}P signals by ^{13}C-labeled and unlabeled glyphosate is reported in Tables 1 and 2, and dephasing of S3P ^{31}P signals in Tables 3−5. The resulting values for internuclear distances are independent of the number of rotor cycles of dephasing (a good measure of reliability), so long as $0.2 < \lambda_{\text{D}} < 0.5$. For the EPSP synthase complexes, when λ_{D} is small (for example, $N_{\text{c}} <$ 56, Table 4), the background makes up such a large fraction of the total dephasing that, with the present sensitivity, the entire analytical approach is suspect. When λ_{D} is large, the separability of powder averaging assumed in eq 4 is questionable. The symptom in this latter situation is a steady

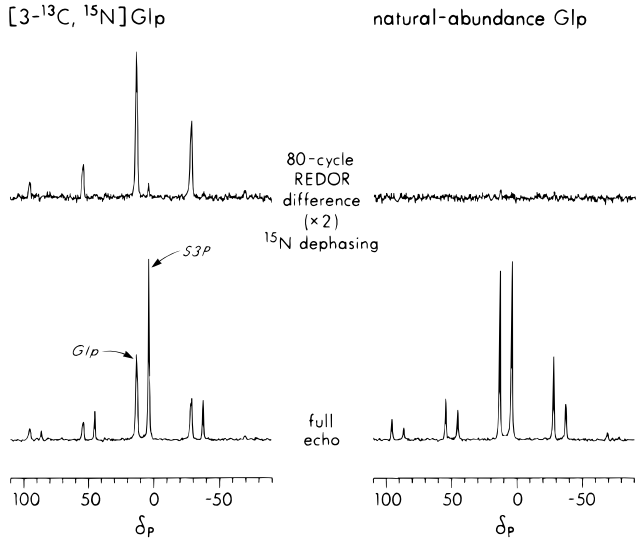

FIGURE 5: REDOR ^{31}P NMR spectra of lyophilized EPSPS−S3P−[3-^{13}C,^{15}N]Glp (left) and EPSPS−S3P−Glp (right) after 80 rotor cycles of ^{15}N dephasing with 5-kHz magic-angle spinning. The REDOR-difference spectrum (top, left) arises primarily from the glyphosate label. The S and S_0 spectra of the labeled Glp complex were each the result of the accumulation of 110 592 scans, while those of the natural-abundance Glp complex were each from 135 168 scans.

Table 1: REDOR Dephasing of Glyphosate ^{31}P by [1-^{13}C]Glyphosate in Ternary Complexes of EPSP Synthase Spinning at the Magic Angle at 5 kHz

N_{c}	$(\Delta S/S_0)_{\text{obsd}}$ (dephasing by label plus background)	$(\Delta S/S_0)_{\text{nat abnd}}$ (dephasing only by background)	λ_{D}[a]	D (Hz)	r (Å)
32	0.346	0.081	0.520	81	5.3
48	0.515	0.169	0.625	65	5.7
64	0.736	0.192	0.794	62	5.8
80	0.830	0.243	0.853	53	6.1

[a] From $\lambda_{\text{D}}^2 = (15/16)(1 - [1 - (\Delta S/S_0)_{\text{obsd}}]/[1 - (\Delta S/S_0)_{\text{nat abnd}}])$.

Table 2: REDOR Dephasing of Glyphosate ^{31}P by [2-^{13}C]Glyphosate in Ternary Complexes of EPSP Synthase Spinning at the Magic Angle at 5 kHz

N_c	$(\Delta S/S_0)_{obsd}$ (dephasing by label plus background)	$(\Delta S/S_0)_{nat\ abnd}$ (dephasing only by background)	λ_D[a]	D (Hz)	r (Å)
8	0.043	0[b]	0.201	125	4.6
16	0.200	0.030	0.405	127	4.5
24	0.360	0.040	0.559	116	4.7
32	0.606	0.081	0.732	114	4.7
40	0.772	0.115	0.834	104	4.9
48	0.803	0.169	0.846	88	5.1[c]
56	0.817	0.193	0.851	76	5.4[c]
64	0.778	0.192	0.825	64	5.7[c]
72	0.861	0.269	0.871	61	5.8[c]
80	0.819	0.243	0.845	53	6.1[c]

[a] From $\lambda_D^2 = (15/16)(1 - [1 - (\Delta S/S_0)_{obsd}]/[1 - (\Delta S/S_0)_{nat\ abnd}])$. [b] By assumption. [c] Not used in error estimate of Table 7.

Table 3: REDOR Dephasing of Shikimate 3-Phosphate ^{31}P by [1-^{13}C]Glyphosate in Ternary Complexes of EPSP Synthase Spinning at the Magic Angle at 5 kHz

N_c	$(\Delta S/S_0)_{obsd}$ (dephasing by label plus background)	$(\Delta S/S_0)_{nat\ abnd}$ (dephasing only by background)	λ_D[a]	D (Hz)	r (Å)
32	0.124	0.111	0.117	18	8.7
48	0.195	0.191	0.068	7	11.9[b]
64	0.249	0.227	0.163	13	9.8
80	0.340	0.278	0.284	18	8.8

[a] From $\lambda_D^2 = (15/16)(1 - [1 - (\Delta S/S_0)_{obsd}]/[1 - (\Delta S/S_0)_{nat\ abnd}])$. [b] Not used in error estimate of Table 7.

Table 4: REDOR Dephasing of Shikimate 3-Phosphate ^{31}P by [2-^{13}C]Glyphosate in Ternary Complexes of EPSP Synthase Spinning at the Magic Angle at 5 kHz

N_c	$(\Delta S/S_0)_{obsd}$ (dephasing by label plus background)	$(\Delta S/S_0)_{nat\ abnd}$ (dephasing only by background)	λ_D[a]	D (Hz)	r (Å)
32	0.132	0.111	0.147	23	8.0[b]
40	0.173	0.152	0.151	19	8.6[b]
48	0.196	0.191	0.079	8	11.3[b]
56	0.289	0.173	0.363	32	7.2
64	0.338	0.227	0.366	29	7.5
72	0.407	0.242	0.451	31	7.2
80	0.447	0.278	0.468	29	7.4

[a] From $\lambda_D^2 = (15/16)(1 - [1 - (\Delta S/S_0)_{obsd}]/[1 - (\Delta S/S_0)_{nat\ abnd}])$. [b] Not used in error estimate of Table 7.

Table 5: REDOR Dephasing of Shikimate 3-Phosphate ^{31}P by [3-^{13}C]Glyphosate in Ternary Complexes of EPSP Synthase Spinning at the Magic Angle at 5 kHz

N_c	$(\Delta S/S_0)_{obsd}$ (dephasing by label plus background)	$(\Delta S/S_0)_{nat\ abnd}$ (dephasing only by background)	λ_D[a]	D (Hz)	r (Å)
32	0.158	0.111	0.222	35	7.0
40	0.243	0.152	0.318	40	6.7
48	0.281	0.191	0.323	34	7.1
56	0.313	0.173	0.399	36	6.9
64	0.332	0.227	0.356	28	7.5
72	0.414	0.242	0.462	32	7.2
80	0.439	0.278	0.457	29	7.5

[a] From $\lambda_D^2 = (15/16)(1 - [1 - (\Delta S/S_0)_{obsd}]/[1 - (\Delta S/S_0)_{nat\ abnd}])$.

upward drift of r with increasing N_c (Tables 1 and 2). Clearly, whenever λ_D is large, we need a more realistic accounting of the background dephasing. We achieve this by construction of a model lattice to position background and label ^{13}C dephasing centers relative to one another. This approach is described in a later section.

Table 6: Motional Reduction of Maximum Expected REDOR Dephasing in Ternary Complexes of EPSP Synthase Spinning at the Magic Angle at 5 kHz

Glp label	N_c	$\Delta S/S_0$ obsd	$\Delta S/S_0$ calcd	motional scale factor	line width[a] (Hz)	T_2[a] (ms)
^{15}N	80	0.91[b]	1.0	1.1	90	14
1-^{13}C	96	0.90[c]	1.0	1.1	100	14
2-^{13}C	56	0.82[d]	1.0	1.2	220	15
2-^{13}C[e]	56	0.74[d]	1.0	1.3	240	16

[a] For the ^{31}P line of S3P. [b] Two-bond coupling between ^{15}N and ^{31}P for [3-^{13}C,^{15}N]Glp. [c] Four-bond coupling between ^{13}C and ^{31}P for [1-^{13}C]Glp. [d] Three-bond coupling between ^{13}C and ^{31}P for [2-^{13}C]Glp. [e] Second of two ternary complexes formed using [2-^{13}C]Glp.

REDOR Dephasing and Molecular Motion. The distance determinations of Tables 1−5 have assumed no motional averaging except for a 5% reduction in D arising from ultrahigh-frequency motions present even in nominally rigid crystals at room temperature (Gullion & Schaefer, 1989a). It is not unreasonable to anticipate additional motions in the lyophilized EPSP synthase ternary complexes, which are, after all, not rigid crystals. We can monitor for the presence of such motions by confirming that full dephasing is observed for relatively strong *intra*molecular dipolar couplings after a sufficiently large number of rotor periods. For example, the geometry-independent two-bond ^{31}P−^{15}N coupling in EPSPS−S3P−[3-^{13}C,^{15}N]Glp is sufficient to result in an almost full ^{31}P $\Delta S/S_0$ after 80 rotor cycles of dephasing with 5-kHz magic-angle spinning (Figure 5, left). A similar ^{31}P observation has been made for the one-bond ^{31}P−^{13}C coupling (data not shown). Thus, significant motion of glyphosate within its binding site for this particular sample is unlikely. However, reduced dipolar couplings for some of the other samples appear to be present. For example, neither of the ternary complexes formed using [2-^{13}C]Glp show the full dephasing expected for any reasonable value of a three-bond ^{13}C−^{31}P coupling (Table 6). In addition, reductions in the maximum obtainable dephasing have a direct correlation with the ^{31}P inhomogeneous line width, suggesting that slight disordering in the binding site may permit additional motion.

To take motion into account rigorously in a quantitative determination of internuclear distances from REDOR dephasing data requires specifying details of the averaging process that is beyond the scope of the present measurements. Instead, we invoke a simple model that appears to be consistent with the available data and permits first-order motional corrections to distance determinations. We assume that S3P is spatially fixed, based on its invariant T_2 (Table 6). Next, we assume that the carboxyl end of glyphosate is also fixed; this assumption is based on the consistency of the carboxyl ^{13}C line width from sample to sample (McDowell et al., 1996). Finally, we assume that at a fraction of binding sites for some of the sample preparations the phosphonate end of glyphosate undergoes sufficiently fast, large-amplitude motions that observable intramolecular coupling to the C-1 and C-2 carbons is eliminated. This fraction is determined by the $\Delta S/S_0$ dephasing plateau and varies from complex to complex between 10% and 30% (Table 6). The motion is assumed to be fast enough to average weak ^{13}C−^{31}P couplings but not fast enough to

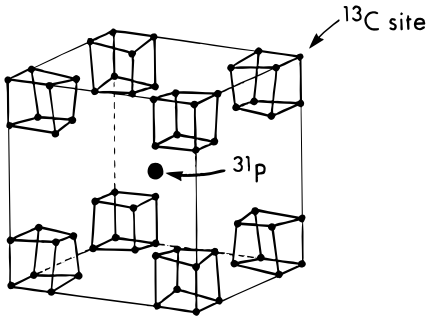

FIGURE 6: Model lattice for the positioning of ^{13}C dephasing centers (small circles) around a central ^{31}P nucleus (big circle). Altogether 64 carbon sites with 8 unique distances can be represented by distortions of the small cubes in the eight corners of the big cube. This drawing shows four unique distances.

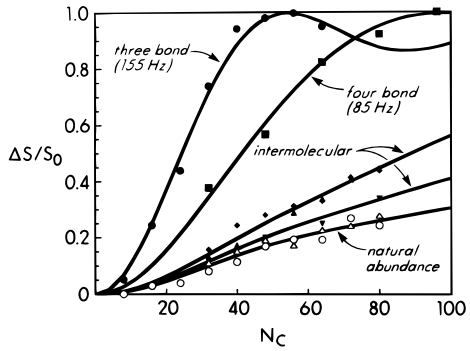

FIGURE 7: REDOR ^{31}P dephasing by ^{13}C for EPSPS−S3P−Glp ternary complexes spinning at the magic angle at 5 kHz. The Glp ^{31}P signals are dephased by [2-^{13}C]Glp (solid circles) and [1-^{13}C]-Glp (solid squares). These values have been scaled to take into account the effects of motion. (See text associated with Table 6.) The S3P ^{31}P signals are dephased by [3-^{13}C]Glp (solid diamonds) [2-^{13}C]Glp (solid triangles), and [1-^{13}C]Glp (inverted solid triangles). The natural-abundance glyphosate complex yields dephasing of the ^{31}P of both S3P (open circles) and Glp (open triangles). The solid curves were calculated using the lattice model of Figure 6 to account for specific $^{31}P-^{13}C$ dipolar couplings of 155, 85, 33, and 20 Hz, respectively, top to bottom, in the presence of the natural-abundance background.

reduce significantly the $^{1}H-^{31}P$ coupling necessary for cross polarization. (We could have equivalently assumed that the phosphonate end of glyphosate was fixed and the carboxyl end wobbled). The net effect of molecular motion therefore is to reduce only intramolecular glyphosate dipolar couplings slightly (and possibly the DRAMA-determined $^{31}P-^{31}P$ couplings), which results in internuclear distances which are systematically too large by 2−9%. Knowledge of the $\Delta S/S_0$ plateaus (Table 6) leads to corrections for most of this overdetermination (*cf.* below).

Lattice−Model Interpretation of Background Dephasing. The natural-abundance ^{13}C nuclei make a significant contribution to the ^{31}P REDOR dephasing (Tables 1−5). An accurate, quantitative accounting of the background dephasing depends on the positions of all ^{13}C spins within 10 Å of the observed ^{31}P nucleus. In the absence of having the exact coordinates, we carried out a simulation for a model lattice containing 64 carbon sites. The locations of these sites with respect to the observed ^{31}P nucleus are shown qualitatively in Figure 6. By identical distortions of the small cubes at each corner of the big cube, we can define up to eight unique $^{31}P-^{13}C$ distances to account for coupling to specific labels.

In our fitting of the experimental EPSP synthase data (Tables 1−5), we distorted the small cubes to produce four distances corresponding to $^{31}P-^{13}C$ dipolar couplings of 155, 85, 33, and 20 Hz, respectively. At the *same* time, the natural-abundance REDOR dephasing (Figure 7, open symbols) was matched by adjusting the dimensions of the big cube using a normalized sum of 64 calculations where one site only is ^{13}C and 2016 ($64 \times 63/2$) calculations where two sites are ^{13}C. All $^{13}C-^{13}C$ couplings are ignored. The weighting factor for each calculation in the sum was determined by assuming a probability of 0.011 that any given site is occupied by ^{13}C. REDOR dephasing due to a single ^{13}C label plus the background ^{13}C (Figure 7, solid symbols) was calculated by fixing one site as occupied by the ^{13}C label and then summing one REDOR dephasing calculation where all other sites are ^{12}C, with 63 calculations where one other site is ^{13}C and 1953 ($63 \times 62/2$) calculations where two other sites are ^{13}C. Adjustment of the big and little cubes was done iteratively to ensure that all the REDOR dephasing results for both background, and label + background, would be matched satisfactorily by the same lattice. Each calculation made use of the general relationship (Boyce, 1972) $\Delta S/S_0 = \langle\cos(\sum_i \Delta\phi_{Di})\rangle = \langle\Pi_i \cos\Delta\phi_{Di}\rangle$, where $\Delta\phi_{Di}$ is the REDOR phase accumulation (Gullion & Schaefer, 1989a) arising from the dipolar coupling between the *S* spin (^{31}P in this instance) and the *i*th member of a collection of *I* spins not interacting with one another (Wang et al., 1984). The *I* spins are the ^{13}C label together with all the background ^{13}C spins. Contributions from lattice configurations with more than two background ^{13}C spins are negligible and were ignored in our calculations. The spatial powder average is easy to perform for a simple product of independent terms (see eq 4) if the positions of all the *I* spins relative to the *S* spin are known, which is the situation for the model lattice. Motional averaging was taken into account for the ^{31}P dephasing of glyphosate by the ^{13}C label of [1-^{13}C]glyphosate by multiplying the experimental values of $\Delta S/S_0$ (Table 1) by the sample-specific scale factor of 1.1 (Table 7) to produce the values used for the fitting (Figure 7, solid squares). A similar procedure was followed for the ^{31}P dephasing of glyphosate by [2-^{13}C]glyphosate using the scale factor of 1.2 (Table 7) to produce the $\Delta S/S_0$ values used for the fitting (Figure 7, solid circles).

Table 7: Dipolar Couplings and Internuclear Distances from Lattice Simulations of REDOR Dephasing in Ternary Complexes of EPSP Synthase

observing nucleus	dephasing nucleus[a]	motional scale factor	D^b (Hz)	r^c (Å)
Glp ^{31}P	1-^{13}C	1.1[d]	85	5.2 ± 0.3
Glp ^{31}P	2-^{13}C	1.2[d]	155	4.2 ± 0.1
S3P ^{31}P	1-^{13}C	1.0[e]	20	8.3 ± 0.6
S3P ^{31}P	2-^{13}C	1.0[e]	33	7.1 ± 0.2
S3P ^{31}P	3-^{13}C	1.0[e]	33	7.1 ± 0.3

[a] In glyphosate. [b] From Figure 7. [c] From fits to experimental $\Delta S/S_0$ as a function of N_c (Tables 1−5, Figure 7); error estimate is standard deviation of most reliable determinations (see footnotes, Tables 2−4). [d] From Table 6. [e] By assumptions for asymmetry of motion (see text).

The model−lattice simulations result in excellent fits to the experimental REDOR data (Figure 7, solid lines). The values of 4.2 and 5.2 Å for the intramolecular distances between the ^{31}P of glyphosate and the C-1 and C-2 carbons, respectively, are slightly shorter than those obtained using the approximation of eq 8 (Tables 1 and 2). In part, this difference is due to the motional corrections made on the data used in the simulations (Figure 7) which increase the

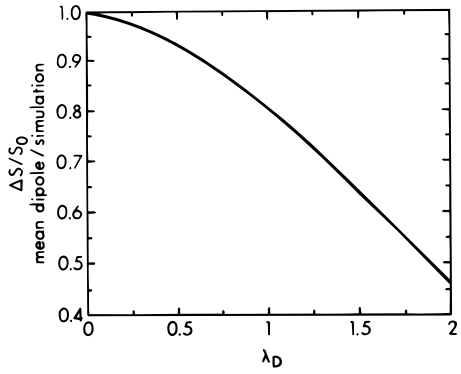

FIGURE 8: Ratio of calculated $\Delta S/S_0$ from eq 8 of the text (mean dipole approximation) to $\Delta S/S_0$ from the lattice simulation model of Figure 6, as a function of $\lambda_D = N_c T_r D$, where N_c is the number of rotor cycles of dephasing, T_r is the rotor period, and D is the dipolar coupling between the observing nucleus and the label. The simulation generated $\Delta S/S_0$ both for the natural-abundance background and for label + background.

Table 8: Internuclear Distances in Energy-Minimized Conformations from Molecular Dynamics Simulations of an S3P−Glp Complex[a]

atom pair	restraint range (Å)	S3P−Glp complex[b] (Glp *t*) (Å)	S3P−Glp complex[b] (Glp g^+) (Å)	S3P−Glp complex[b] (Glp g^-) (Å)
Glp P−Glp C1	4.9−5.5	5.2	4.8	4.8
Glp P−Glp C2	4.1−4.3	4.1	4.1	4.1
S3P P−Glp C1	7.7−8.9	7.7−8.6	7.7−8.5	7.7−8.6
S3P P−Glp C2	6.9−7.3	6.9−7.4	6.9−7.3	6.9−7.3
S3P P−Glp C3	6.8−7.4	6.8−7.4	6.8−7.4	6.8−7.4
S3P P−Glp P	7.5−9.5	7.5−8.5	7.5−8.5	7.5−8.5
S3P P−Glp N	7.0−9.0	7.0- 8.0	7.0−7.9	7.0−7.8

[a] Single numbers indicate that the values varied by less than ±0.05 Å. [b] Simulations of the S3P−Glp complex were restrained to the experimentally determined distance ranges cited in column 2. Only complexes in which the 3-phosphate of S3P was axial were considered.

dipolar couplings and shorten the distances. However, theoretical comparisons of the use of eq 8 and the lattice simulation (Figure 8), show a consistent underestimate of $\Delta S/S_0$ (and hence overestimate of r) by the use of eq 8. The intermolecular distances obtained by the lattice simulation are also slightly less than those obtained by the use of eq 8.

The symmetry of the lattice allowed a considerable reduction in the actual number of REDOR dephasing calculations that were performed. We believe that lattice calculations of this type will be generally useful whenever contributions to the REDOR dephasing from background nuclei are sizable. If the REDOR-determined distances ultimately lead to a determination of the lattice positions, a refinement of the background contribution to dephasing should be possible. In the absence of a lattice calculation, we believe that the average dipolar approximation of eq 8, with the overestimate of r corrected using the λ_D dependence of Figure 8, is adequate to determine distances.

Molecular Modeling of the Interligand Geometry. To characterize the geometry of S3P and Glp when bound to EPSP synthase, the internuclear distances measured by DRAMA and REDOR NMR were used as restraints in molecular dynamics simulations of S3P and Glp complexes. The results are summarized in Table 8. These simulations produced half-chair conformations of S3P in which the phosphate was either axial or equatorial. Both molecular modeling studies *in vacuo* and solution NMR studies indicate that S3P prefers a half-chair conformation with the phosphate in an axial position (Castellino et al., 1991). Transferred NOE studies show the bound conformation of S3P in the ternary complex with the enzyme and Glp to be the same as the solution conformation (Leo et al., 1992). Consequently, only structures of the S3P−Glp complex in which S3P adopts this preferred conformation are reported in Table 8. The results reveal that Glp bound to EPSP synthase is for the most part fully extended. Most of the complexes observed had all torsion angles in the *trans* conformation (Table 8). Some complexes were observed in which the C1−C2−N−C3 conformation was either g^+ or g^-. In these structures, the observed C1−P intramolecular distance is slightly shorter (4.8 Å) than the range measured by REDOR (4.9−5.5 Å). All three Glp conformations are consistent with previous solution ^{31}P NMR studies which concluded that Glp is not bound to EPSP synthase in a spirocyclic, internally H-bonded conformation (Castellino et al., 1989). X-ray analysis of Glp in zwitterion form (Knuuttila & Knuuttila, 1979) reveals a structure similar to the g^- conformation seen here, while the crystal structure of the calcium salt (Smith & Raymond, 1988) is closer to the fully extended conformer.

When complexes produced from the restrained molecular dynamics simulations of S3P and Glp are overlaid using S3P as the fixed reference, Glp exhibits little preference in spatial position (data not shown). Given that all of the experimental restraints on S3P involve a single atom, this is not suprising. (A preferred orientation is achieved when REDOR distance constraints from S3P and Glp to protein side chains are imposed; this is the fourth part of the analysis strategy outlined in the introduction). However, when the complexes are overlaid using Glp as the fixed reference, it is clear that the DRAMA and REDOR distance restraints require that only one side of Glp face S3P. In Figure 9, S3P−Glp complexes (*trans* Glp only) have been overlaid using the atoms of Glp as a reference. The arc of points surrounding the central Glp represents the position adopted by the S3P phosphorus in each of the complexes. For clarity, only a few selected orientations of S3P are shown. In this presentation it is clear that the restraints, which require C2 and C3 to be closer to S3P than the other atoms of Glp, force the hydrogens of the Glp nitrogen to be oriented away from S3P. A proposed hydrogen-bonding interaction between the amino group of Glp and a hydroxyl of S3P (Anderson & Johnson, 1990) is unlikely in this geometry. When the conformations of Table 8 were screened using standard hydrogen bond geometries as criteria (Taylor & Kennard, 1984), only 16 of about 500 complexes were found to have an S3P O5−Glp N distance less than 3.2 Å, and none had an S3P O4−Glp N distance in this range.

Efforts to develop more potent forms of Glp by chemical modification have been largely unsuccessful (Knowles et al., 1993). Notably, alkyl substituents at C2 and C3 increase the IC_{50} of glyphosate from 2 μM to more than 80 mM, although the impact of substitution at N can be less and is in some cases minor. *N*-Methylglyphosate, *N*-aminoglyphosate, and *N*-hydroxyglyphosate exhibit $K_{i(app)}$ vs PEP of 78, 0.61, and 2.2 μM, respectively, compared to a $K_{i(app)}$ vs PEP of 0.16 μM for glyphosate. One explanation for these findings is that the additional steric bulk of moieties at C2 and C3 would have to occupy space between S3P and Glp. For some of the complexes generated in these calculations, there is not sufficient space between the two ligands to

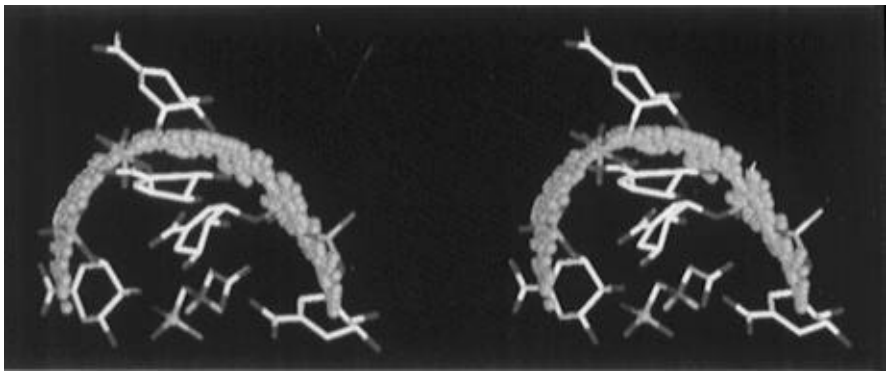

FIGURE 9: Crossed stereoview of S3P−Glp complexes generated by molecular dynamics simulations using seven inter- and intraligand distances from DRAMA and REDOR measurements as restraints. Atoms of Glp in each S3P−Glp complex are overlaid. The arc of yellow points surrounding Glp represents the location of the S3P phosphorus atom in each complex. For clarity, only a few orientations of the entire S3P molecule are shown. The only hydrogens displayed are those on the nitrogen of Glp. Color code: white, carbon; yellow, phosphorus; red, oxygen; blue, nitrogen; cyan, hydrogen.

accommodate additional steric bulk.

Glyphosate as a Transition-State Analog. Glp has been proposed as a transition-state analog for EPSP synthase (Anton et al., 1983; Steinrucken & Amrhein, 1984a) in which the positively charged nitrogen emulates the nascent positive charge of PEP, while the carboxy and phosphonate groups mimic the corresponding groups of PEP. A tetrahedral intermediate (**1R** or **1S**, Figure 3) formed from S3P and PEP has both been isolated and observed bound to the enzyme (Anderson et al., 1990, 1988b). It is unknown if the newly formed chiral center in this intermediate is *R* or *S*. A ketal byproduct isolated from enzyme incubations supports the *S* configuration (Leo et al., 1990). The corresponding phosphonate analogs (**2R** and **2S**, Figure 3) of the tetrahedral intermediate have nanomolar affinities (Alberg & Bartlett, 1989; Alberg et al., 1992). The greater potency of the *R* phosphonate argues for an *R* configuration in the tetrahedral intermediate.

Several key functional groups of intermediate **1** such as CO_2 and PO_4 are essential for the binding of S3P and PEP to EPSP synthase, while the newly formed chiral center of **1** approximates the location of charge development during catalysis. Thus, the range of internuclear distances between these sites over all possible conformations of **1** provides limits on the geometry of S3P and PEP when bound to the enzyme. Inhibitor **2** is derived from **1**, contains the same sites of interest, has a high affinity for the enzyme, and should also serve as a reasonable estimator of the geometry of S3P and PEP when bound. Unrestrained molecular dynamics simulations of **1** and **2** were performed and the resulting energy-minimized conformations used to determine the minimum and maxiumum interatomic distances between the two phosphorus atoms, the CO_2 carbon (PEP portion only), and the new chiral center (or its equivalent in **2**). These distances were then compared with the analogous DRAMA and REDOR-determined distances measured in the EPSPS−S3P−Glp ternary complex to assess the degree of similarity of the bound geometries of Glp and PEP. The results of the simulations are summarized in Table 9. Internuclear distances were initially tabulated separately for the 3-axial and 3-equatorial shikimate ring conformers of each inhibitor (data not shown). Because there was little difference between the two sets of numbers, and there is no evidence that either is preferred when bound to EPSP synthase, the reported ranges include all conformers.

Table 9: Internuclear Distance Ranges Observed in Conformers Generated from Molecular Dynamics Simulations of the Tetrahedral Intermediate of EPSP Synthase and Its Phosphonate Analog

atom pair	*R*-tetrahedral intermediate (**1R**)[a] (Å)	*S*-tetrahedral intermediate (**1S**)[a] (Å)	*R*-phosphonate (**2R**)[b] (Å)	*S*-phosphonate (**2S**)[b] (Å)
PEP P−PEP CO_2	3.0−4.0	3.1−4.1	2.6−2.8	2.6−2.8
S3P P−PEP CO_2	4.4−8.2	4.8−8.1	4.3−7.8	4.5−8.1
S3P P−PEP P	4.7−9.3	4.4−8.8	4.6−8.4	4.8−8.2
S3P P−PEP C2	5.2−7.7	4.8−7.1	5.0−7.0	5.3−7.1

[a] Structure **1**, Figure 3. [b] Structure **2**, Figure 3.

Conformers of the EPSP synthase tetrahedral intermediate (**1R** or **1S**) and its phosphonate analog (**2R** or **2S**) have intramolecular internuclear distances that are largely similar (Table 9), with the exception of the PEP P to CO_2 C distances (3.0−4.1 and 2.6−2.8 Å, respectively). These differences are a consequence of the different number of atoms linking the two groups in **1** and **2** (Figure 3). All of the PEP P to CO_2 C distances are significantly shorter than the analogous Glp C1 to P REDOR distance (4.9−5.5 Å) because fewer atoms link these centers in **1** and **2** than in Glp. Only a few conformers of **1R**, **1S**, **2R**, and **2S** (10 of 147, 6 of 122, 2 of 92, and 3 of 79, respectively) had S3P P−PEP C2 distances in the range of the analogous experimentally measured S3P P−Glp N distance (7.0−9.0 Å). The P−P internuclear distances observed in these molecules were a better match to the S3P P−Glp P DRAMA measurement in the ternary complex (69, 36, 26, and 23 conformers, respectively), and a small number of conformers had S3P P−PEP CO_2 C distances in the range of the analogous S3P P−Glp C1 measurement (32, 16, 12, and 14 conformers, respectively). For most of these molecules, a small number of conformations (14, 11, 0, and 3 for **1R**, **1S**, **2R**, and **2S**, respectively) could simultaneously satisfy the experimental S3P P−Glp P and S3P P−Glp C1 distance ranges. When the REDOR S3P P−Glp N distance was applied as an additional filter, only a handful of conformations remained (5, 1, 0, and 3 for **1R**, **1S**, **2R**, and **2S**, respectively). In every case, these were high-energy conformers, more than 6.5 kcal/mol above the global minimum. A similar analysis of a bisubstrate analog of S3P−Glp (**3**, Figure 3) reveals that the geometry of S3P and Glp when bound to EPSP synthase is not well reproduced (data not shown). An inability to attain the distances which link groups essential for tight binding of S3P and Glp may explain the disappointingly low affinity

of **3** ($K_{i(app)} = 7.4$ μM vs EPSP; Marzabadi et al., 1992), which appears not to interact with the Glp phosphonate binding site.

Our modeling results are inconsistent with the proposed role of Glp as a transition-state or intermediate analog. It has been hypothesized that Glp fits into the PEP binding site by adopting a pinched conformation, in which the two ends of the molecule are folded in toward the Glp N. This type of compact structure would compensate for the extra two atoms which link the terminal functional groups of Glp when compared to PEP. However, all of our molecular dynamics simulations, restrained by DRAMA and REDOR-determined distances measured in the EPSPS−S3P−Glp ternary complex, reveal that Glp adopts extended rather than compact conformations. In addition, we have found no low-energy conformers of intermediate **1** and inhibitor **2** which have internuclear distances that match the analogous distances in the ternary complex. We therefore conclude that the geometry of S3P and PEP when bound to EPSP synthase has little in common with the geometry of S3P and Glp bound to the enzyme. This conclusion is supported by the results of recent fluorescence titration studies which suggest that Glp is unlikely to act as either a transition-state analog or an intermediate analog (Sammons et al., 1995).

REFERENCES

Abell, C., Allen, F. H., Bugg, T. D. H., Doyle, M. J., & Raithby, P. R. (1988) *Acta Crystallogr. Sect. C 44*, 1204−1207.

Alberg, D. G., & Bartlett, P. A. (1989) *J. Am. Chem. Soc. 111*, 2337−2338.

Alberg, D. G., Lauhon, C. T., Nyfeler, R., Fassler, A., & Bartlett, P. A. (1992) *J. Am. Chem. Soc. 114*, 3535−3546.

Anderson, K. S., & Johnson, K. A. (1990) *Chem. Rev. 90*, 1131−1149.

Anderson, K. S., Sikorski, J. A., & Johnson, K. A. (1988a) *Biochemistry 27*, 1604−1610.

Anderson, K. S., Sikorski, J. A., Benesi, A. J., & Johnson, K. A. (1988b) *J. Am. Chem. Soc. 110*, 6577−6579.

Anderson, K. S., Sammons, R. D., Leo, G. C., Sikorski, J. A., Benesi, A. J., & Johnson, K. A. (1990) *Biochemistry 29*, 1460−1465.

Anton, D. L., Hedstrom, L., Fish, S. M., & Abeles, R. H. (1983) *Biochemistry 22*, 5903−5908.

Beusen, D. D., McDowell, L. M., Schmidt, A., Cohen, E. R., & Schaefer, J. (1994) in *Peptides: Chemistry, Structure, and Biology* (Hodges, R. S., & Smith, J., Eds.) pp 760−762, ESCOM, Leiden.

Boyce, J. B. (1972) Thesis, University of Illinois, Urbana-Champaign, p 28.

Castellino, S., Leo, G. C., Sammons, R. D., & Sikorski, J. A. (1989) *Biochemistry 28*, 3856−3868.

Castellino, S., Leo, G. C., Sammons, R. D., & Sikorski, J. A. (1991) *J. Org. Chem. 56*, 5176−5181.

Christensen, A. M., & Schaefer, J. (1993) *Biochemistry 32*, 2868−2873.

Clark, M., Cramer, R. D., III, & Van Opdenbosch, N. (1989) *J. Comput. Chem. 10*, 982−1012.

Gullion, T., & Schaefer, J. (1989a) *J. Magn. Reson. 81*, 196−200.

Gullion, T., & Schaefer, J. (1989b) *Adv. Magn. Reson. 13*, 57−83.

Gullion, T., & Schaefer, J. (1991) *J. Magn. Reson. 92*, 439−442.

Gullion, T. G., Baker, D. B., & Conradi, M. S. (1990) *J. Magn. Reson. 89*, 479−484.

Hing, A. W., Tjandra, N., Cottam, P. F., Schaefer, J., & Ho, C. (1994) *Biochemistry 33*, 8651−8661.

Holl, S. M., McKay, R. A., Gullion, T., & Schaefer, J. (1990) *J. Magn. Reson. 89*, 620−626.

Holl, S. M., Marshall, G. R., Beusen, D. D., Kociolek, K., Redlinski, A. S., Leplawy, M. T., McKay, R. A., Vega, S., & Schaefer, J. (1992) *J. Am. Chem. Soc. 114*, 4830−4833.

Klug, C. A., Zhu, W., Merritt, M. E., & Schaefer, J. (1994) *J. Magn. Reson. 189*, 134−136.

Knowles, W. S., Anderson, K. S., Andrew, S. S., Phillion, D. P., Ream, J. E., Johnson, K. A., & Sikorski, J. A. (1993) *Bioorg. Med. Chem. Lett. 3*, 2863−2868.

Knuuttila, P., & Knuuttila, H. (1979) *Acta Chem. Scand. B 33*, 623−626.

Leo, G. C., Sikorski, J. A., & Sammons, R. D. (1990) *J. Am. Chem. Soc. 112*, 1653−1654.

Leo, G. C., Castellino, S., Sammons, R. D., & Sikorski, J. A. (1992) *Bioorg. Med. Chem. Lett. 2*, 151−154.

Marshall, G. R., Beusen, D. D., Kociolek, K., Redlinski, A. S., Leplawy, M. T., Pan, Y., & Schaefer, J. (1990) *J. Am. Chem. Soc. 112*, 963−966.

Marzabadi, M. R., Font, J. L., Gruys, K. J., Pansegrau, P. D., & Sikorski, J. A. (1992) *Bioorg. Med. Chem. Lett. 2*, 1435−1440.

McDowell, L. M., Schmidt, A., Christenson, A. M., Beusen, D. D., & Schaefer, J. (1993) in 34th Experimental NMR Conference, St. Louis, MO.

McDowell, L. M., Schmidt, A., Cohen, E. R., Studelska, D. R., & Schaefer, J. (1996) *J. Mol. Biol. 256*, 160−171.

Mueller, K. T. (1995) *J. Magn. Reson. A 113*, 81−93.

Mueller, D. D., Schmidt, A., Pappan, K. L., McKay, R. A., & Schaefer, J. (1995) *Biochemistry 34*, 5597−5603.

Sammons, R. D., Gruys, K. J., Anderson, K. S., Johnson, K. A., & Sikorski, J. A. (1995) *Biochemistry 34*, 6433−6440.

Schaefer, J. (1995) in *Stable Isotope Applications in Biomolecular Structure and Mechanisms*, Document LA-12893-C, pp 197−207, National Technical Information Service, U.S. Department of Commerce.

Smith, P. H., & Raymond, K. N. (1988) *Inorg. Chem. 27*, 1056−1061.

Stallings, W. C., Abdel-Meguid, S. S., Lim, L. W., Shief, H. S., Dayringer, H. E., Leimgruber, N. K., Stegman, R. A., Anderson, K. S., Sikorski, J. A., Padgette, S. R., & Kishore, G. M. (1991) *Proc. Nat. Acad. Sci. (U.S.A.) 88*, 5046−5050.

Steinrucken, H. C., & Amrhein, N. (1984a) *Eur. J. Biochem. 143*, 341−349.

Steinrucken, H. C., & Amrhein, N. (1984b) *Eur. J. Biochem. 143*, 351−357.

Studelska, D. R., Klug, C. A., Beusen, D. D., McDowell, L. M., & Schaefer, J. (1996) *J. Am. Chem. Soc.* (submitted for publication).

Taylor, R., & Kennard, O. (1984) *Acc. Chem. Res. 17*, 320−326.

Wang, P. K., Slichter, C. P., & Sinfelt, J. H. (1984) *Phys. Rev. Lett. 53*, 82−86.

BI9529059